Alpha transfer to ^{23}Na

H. T. Fortune,* J. R. Powers,† R. Middleton, and K. Bethge‡
Physics Department, University of Pennsylvania, Philadelphia, Pennsylvania 19104

A. A. Pilt

Nuclear Physics Laboratory, Keble Road, Oxford, England
(Received 23 February 1978)

The ^{19}F(^{6}Li, d)^{23}Na reaction has been investigated at a bombarding energy of 16.0 MeV, using an SF_6 gas target. Angular distributions were measured for all states below 6 MeV excitation and analyzed with zero range distorted-wave Born approximation to extract relative α-spectroscopic factors. These are in very poor agreement witn predictions of a pure SU(3) model calculation and also with a more realistic shell-model calculation.

[NUCLEAR REACTIONS ^{19}F(^{6}Li, d), E = 16.0 MeV; measured $\sigma(E_d, \theta)$. ^{23}Na deduced levels, L, J^π, S_α. SF_6 gas target. Comparison with SU(3), shell model.]

I. INTRODUCTION

Several investigations[1,2] of the (^{6}Li, d) reaction on a number of target nuclei have concluded that the reaction mechanism is one of direct transfer of an α particle, at least for the strongly populated states. Thus, the (^{6}Li, d) reaction provides a technique for measuring α-particle spectroscopic factors. It is superior to the (^{7}Li, t) reaction in at least two respects, both having to do with the $L = 1$ nature of the $\alpha + t$ relative motion in ^{7}Li: (1) the (^{6}Li, d) angular distributions are more characteristic of the final-state J^π than are those in (^{7}Li, t); and (2) zero-range distorted-wave Born approximation (DWBA) calculations have proven to be adequate, whereas (^{7}Li, t) analysis requires finite-range DWBA.

Calculational techniques in nuclear-structure work have advanced to the stage that α-particle spectroscopic factors can frequently be computed for shell-model wave functions. The combined experimental and theoretical work at Rochester has pioneered experimental tests of these calculated S_α's for a number of nuclei.

The nuclear structure of ^{23}Na has been investigated by the use of a wide range of reactions.[3-7] These studies have firmly established the deformed character of ^{23}Na and have provided substantial experimental information concerning the positive- and negative-parity rotational bands.[3,8] Most of the levels below 6 MeV excitation now have unique J^π assignments,[7] and have been placed into rotational bands[8] having $K^\pi = \frac{3}{2}^+$, $\frac{1}{2}^+$, $\frac{1}{2}^-$, and $\frac{1}{2}^+$, as depicted in Fig. 1.

Theoretical α-particle spectroscopic factors (Table I) have been calculated by Draayer[9] for the positive-parity bands, for states characterized by a single irreducible representation $(\lambda\mu)$ of SU(3) and orthogonalized K-projection label, K_j. We have used the ^{19}F(^{6}Li, d) reaction to obtain experimental S_α's. We have also carried out a more realistic SU(3) shell-model calculation (including those representations which are important for α-spectroscopic factors) to obtain wave functions and S_α's for ^{23}Na states.

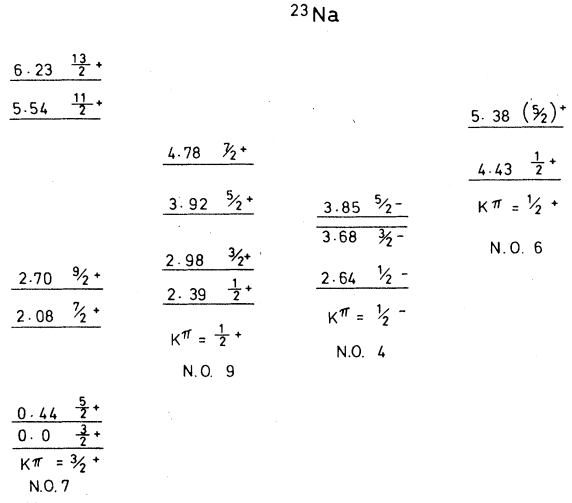

FIG. 1. Rotational bands in ^{23}Na.

TABLE I. Theoretical S_α for $^{19}F \rightarrow {}^{23}Na$, from Ref. 9.

$(\lambda\mu)$	K^π	J^π	L	S_α(rel)
(83)	$\frac{3}{2}^+$	$\frac{3}{2}^+$	2	1.00
		$\frac{5}{2}^+$	2	3.38
		$\frac{7}{2}^+$	4	2.29
		$\frac{9}{2}^+$	4	5.83
		$\frac{11}{2}^+$	6	0.89
		$\frac{13}{2}^+$	6	2.67
(83)	$\frac{3}{2}^+$	$\frac{1}{2}^+$	0	0.00
		$\frac{3}{2}^+$	2	3.75
		$\frac{5}{2}^+$	2	1.37
		$\frac{7}{2}^+$	4	6.53
		$\frac{9}{2}^+$	4	2.98
		$\frac{11}{2}^+$	6	3.36
		$\frac{13}{2}^+$	6	1.59
(64)	$\frac{3}{2}^+$	$\frac{3}{2}^+$	2	0.14
		$\frac{5}{2}^+$	2	0.03
		$\frac{7}{2}^+$	4	1.22
		$\frac{9}{2}^+$	4	0.82
		$\frac{11}{2}^+$	6	2.99
		$\frac{13}{2}^+$	6	3.79
(64)	$\frac{1}{2}^+$	$\frac{1}{2}^+$	0	6.67
		$\frac{3}{2}^+$	2	3.52
		$\frac{5}{2}^+$	2	3.52
		$\frac{7}{2}^+$	4	0.28
		$\frac{9}{2}^+$	4	0.28
		$\frac{11}{2}^+$	6	0.39
		$\frac{13}{2}^+$	6	0.39
(83)	$\frac{5}{2}^+$	$\frac{5}{2}^+$	2	0.00
		$\frac{7}{2}^+$	4	0.08
		$\frac{9}{2}^+$	4	0.03
		$\frac{11}{2}^+$	6	0.84
		$\frac{13}{2}^+$	6	0.63
(64)	$\frac{5}{2}^+$	$\frac{5}{2}^+$	2	0.11
		$\frac{7}{2}^+$	4	0.67
		$\frac{9}{2}^+$	4	1.07
		$\frac{11}{2}^+$	6	3.98
		$\frac{13}{2}^+$	6	3.19

II. EXPERIMENTAL PROCEDURE AND RESULTS

The experiment was performed with 16 MeV $^6Li^{+++}$ ions from the University of Pennsylvania tandem accelerator. The outgoing deuterons were momentum analyzed in a multiangle spectrograph and detected on 25 μm NTA nuclear emulsion plates. Absorbers 0.03 cm in thickness, placed directly in front of the focal planes, prevented particles with $Z>1$ from striking the emulsions. Spectra were recorded in $7\frac{1}{2}^\circ$ angular intervals, beginning at $7\frac{1}{2}^\circ$.

The target was SF_6 gas enclosed in a differentially pumped gas cell with no entrance window. The details of the gas cell system are described elsewhere.[10] The pressure in the cell was maintained at 4 Torr, which corresponds to a target thickness of approximately 30.9 $\mu g/cm^2$. Contamination of the target gas by the usual sources (carbon, nitrogen, and oxygen) was minor because of the purity of the SF_6 ($\geq$ 99.8%) and the nonrecirculation of the gas. Since the cross sections for (^{6}Li, d) reactions drop radically with increases of the target mass, the one-part-in-seven presence of ^{32}S caused no significant problem. For these reasons no impurity groups are apparent in the deuteron spectrum (Fig. 2).

The states in ^{23}Na are identified by the level numbers and excitation energies obtained in the $^{22}Ne(^3He, d)$ reaction.[3] Because of the absence of a reliable calibration at high field settings (63 MHz), excitation energies obtained in the (^{6}Li, d) study had uncertainties of no less than $\pm$25 keV.

Additional difficulty was encountered because of distortion in the spectrograph magnets induced by the high field setting used. As seen in the spectrum, the resolution degenerated with increasing plate distance, or deuteron energy, varying from a value of 26 keV FWHM (full width at half maximum) at high excitation to a value of 47 keV for the ground state, preventing some levels from being resolved. However, most of the levels below 6 MeV excitation are sufficiently separated so that they were resolved.

Differential cross sections were obtained in 7.5° steps for laboratory angles from 7.5° to 52.5° for all states listed in Table II. Angular distributions are displayed in Figs. 3–7.

III. ANALYSIS

Angular distributions were analyzed with the zero-range DWBA code DWUCK,[11] assuming cluster transfer. Optical-model and bound-state parameters are listed in Table III. Except for a slight change in W', the ^{6}Li parameters are those obtained in an analysis of $^{19}F + {}^6Li$ elastic scatter-

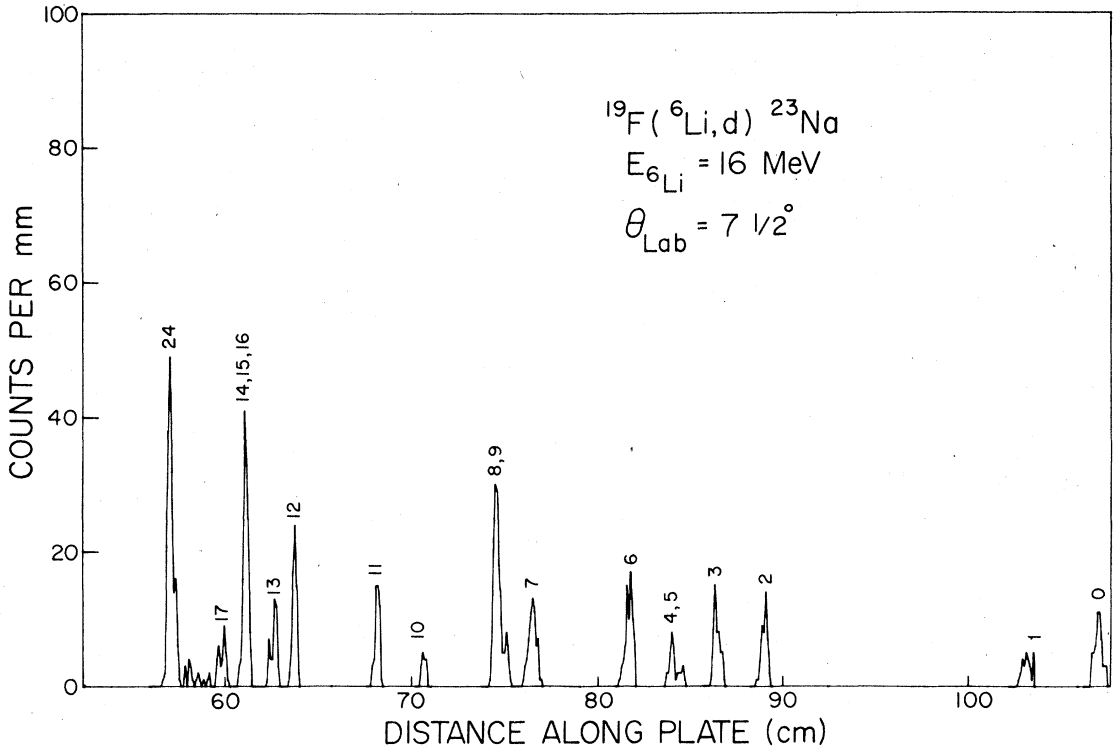

FIG. 2. Spectrum of the ^{19}F(^{6}Li,d)^{23}Na reaction at a bombarding energy of 16.0 MeV and θ_{lab}=7.5°. Level numbers correspond to those in Table II.

TABLE II. Results of the ^{19}F(^{6}Li, d)^{23}Na reaction for states with known structure.

Group[a]	E_x[a] (MeV)	E_x[b] (MeV)	J^π[b]	K^π	$N-1;L$	S_α(rel) Exp.	S_α(rel) Theory
0	0.0	0.0	$\frac{3}{2}^+$	$\frac{3}{2}^+$	3;2	1.00[c]	1.00[c]
1	0.439	0.440	$\frac{5}{2}^+$	$\frac{3}{2}^+$	3;2	0.40	3.38
2	2.078	2.076	$\frac{7}{2}^+$	$\frac{3}{2}^+$	2;4	1.98	2.29
3	2.392	2.391	$\frac{1}{2}^+$	$\frac{1}{2}^+_1$	4;0	4.0	0.0
4	2.642	2.640	$\frac{1}{2}$	$\frac{1}{2}^-$	3;1	0.27	···
5	2.704	2.704	$\frac{9}{2}^+$	$\frac{3}{2}^+$	2;4	0.66	5.83
6	2.983	2.982	$\frac{3}{2}^+$	$\frac{1}{2}^+_1$	3;2	0.85	3.75
7	3.679	3.678	$\frac{3}{2}^-$	$\frac{1}{2}^-$	3;1	0.50	···
8	3.852	3.848	$\frac{5}{2}^-$	$\frac{1}{2}^-$	2;3	(<2.5)	···
9	3.918	3.915	$\frac{5}{2}^+$	$\frac{1}{2}^+_1$	3;2	(1.12)	1.37
10	4.435	4.432	$\frac{1}{2}^+$	$\frac{1}{2}^+_2$	4;0	0.54	6.67
11	4.777	4.776	$\frac{7}{2}^+$	$\frac{1}{2}^+_1$	2;4	1.44	6.53
12	5.378	5.380	$(\frac{5}{2})^+$	$(\frac{1}{2}^+_2)$	3;2	0.34	3.52
13	5.536	5.536	$\frac{11}{2}^+$	$\frac{3}{2}^+$	1;6	(1.84)	0.89

[a]Reference 3.
[b]Reference 7.
[c]Normalized.

ing.[12] The deuteron parameters are those used in the earlier analysis[3] of ^{22}Ne(^{3}He, d)^{23}Na, which has the same exit channel. For the positive-parity final states the $\alpha + {}^{19}$F radial wave function was chosen to have eight quanta of excitation, i.e., $2(N-1)+L=8$, where $N-1$ is the number of radial nodes (discounting the ones at 0 and ∞). Since the low-lying negative-parity states are dominantly of the structure $(sd)^8(1p_{1/2})^{-1}$, transfer to them was computed assuming transfer of 7 quanta to the 5p2h components of the ^{19}F g.s. Of course, if these are pure hole states, their population is forbidden in the absence of core excitation in the ^{19}F(g.s.). This core excitation is small, but not zero. An $(sd)^3 + 5p2h$ shell model calculation for ^{19}F [Pilt, (unpublished)] predicts ~2% core excitation in the ground state. The low-lying negative-parity states are weak, as expected.

Because ^{19}F has $J^\pi = \frac{1}{2}^+$, each final state is reached by a unique L value. Furthermore this L value must be numerically equal to the l value observed[3] in ^{22}Ne(^{3}He, d) to the same final state.

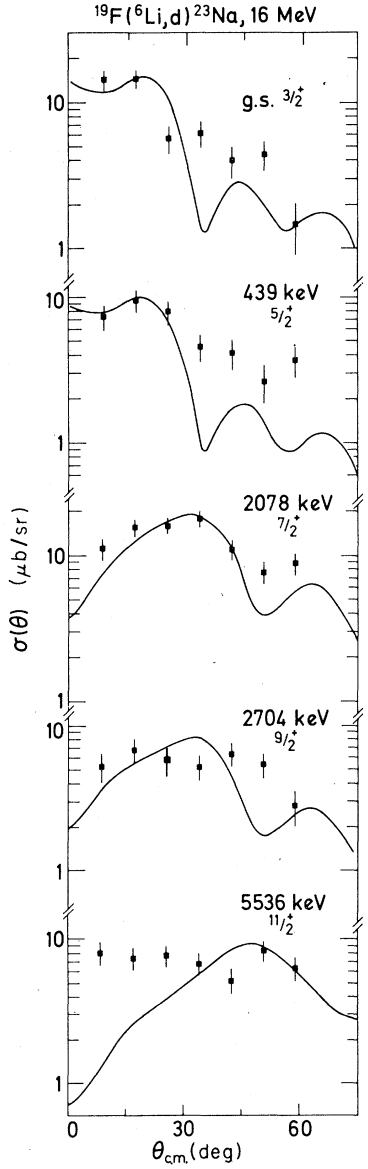

FIG. 3. Angular distributions for the ^{19}F(^{6}Li, d)^{23}Na reaction populating members of the g.s. band. Curves are results of DWBA calculations, as described in the text. Relative spectroscopic factors are listed in Table II.

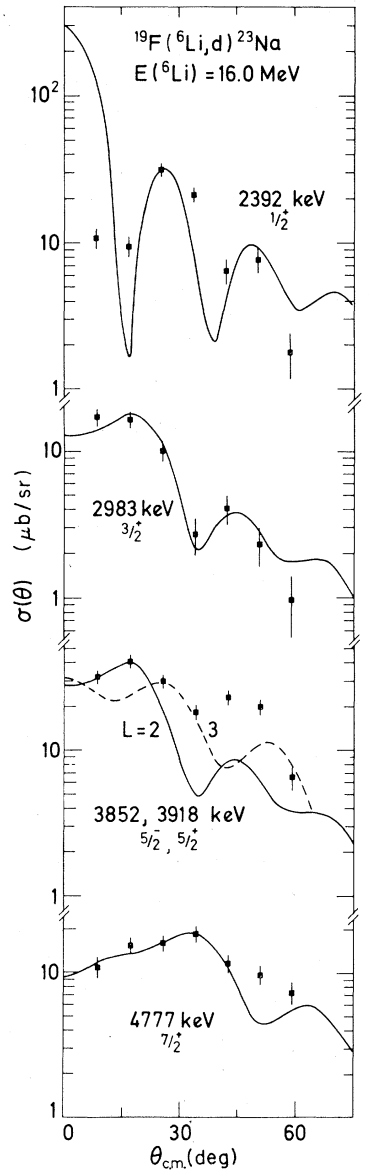

FIG. 4. Same as Fig. 3, but for members of the first $\frac{1}{2}^+$ band.

Thus, even for those few states without a unique J^π assignment, but with an l assignment in (^{3}He, d), the L value is known.

α-particle spectroscopic factors S_α were extracted by normalizing the DWBA curves to the data at angles near where the cross section is a maximum, making use of the expression

$$\sigma_{\text{exp}}(\theta) = \left(\frac{2J_f+1}{2J_i+1}\right) N S_\alpha \frac{\sigma_{\text{DW}}(\theta)}{2L+1}.$$

Since the normalization factor N is not known for the (^{6}Li, d) reaction, we have normalized the g.s. S_α to unity. All other S_α's are relative to this value. We believe these relative spectroscopic factors are accurate to about ±30% for the states whose angular distributions are well fitted.

Angular distributions for members of the g.s. band are displayed in Fig. 3. The DWBA fits are reasonable except for the $\frac{11}{2}^+$ state. The difference between $L = 2$ and 4 shapes is well accounted for by the calculations. Resulting spectroscopic factors are listed in Table II. Also listed there are theoretical S_α's from Draayer.[9] An "odd-even" effect is observed in the experimental values of S_α—the spectroscopic factor for the $\frac{3}{2}^+$ g.s. is significantly larger than that for the $\frac{5}{2}^+$ 0.44-MeV state, and that for the $\frac{7}{2}^+$ 2.08-MeV level is significantly larger than that for the $\frac{9}{2}^+$ 2.70-MeV state. The spectroscopic factor for the $\frac{11}{2}^+$ state is probably not very reliable because of the poor fit to its angular distribution. The $\frac{13}{2}^+$ state is too weak to be observed. If it were as strong as the $\frac{11}{2}^+$ state, it would have been observed.

Draayer's spectroscopic factors[9] (listed in Table I) also possess an odd-even effect, *but in the opposite direction.* For each L value, within the g.s. band, the spectroscopic factor for $J = L + \frac{1}{2}$ is predicted to be significantly larger than that for $J = L - \frac{1}{2}$. The $\frac{5}{2}^+$ to $\frac{9}{2}^+$ ratio is well accounted for, as is the $\frac{3}{2}^+ : \frac{7}{2}^+ : \frac{11}{2}^+$ ratio. The simple SU(3) model thus appears to get wrong the J splitting of strength. Mixing of different SU(3) configurations with $K^\pi = \frac{3}{2}^+$ could reduce the discrepancy (because of alternating phases), but no reasonable amount of mixing gives good agreement. The results of a more realistic calculation are discussed

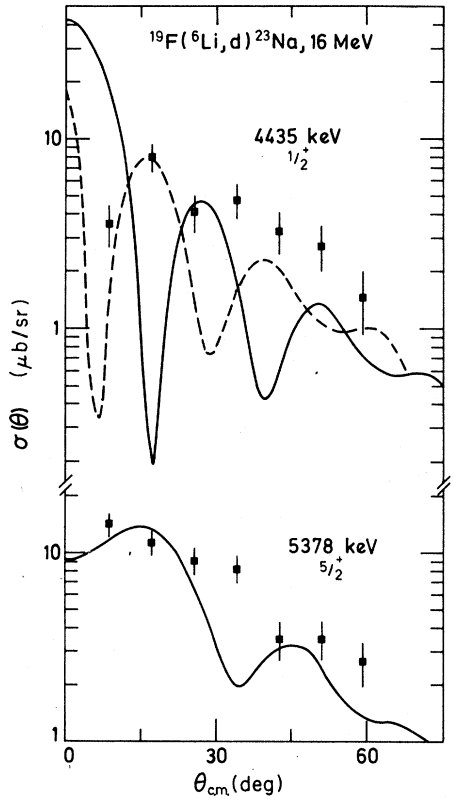

FIG. 5. Same as Fig. 3, but for two members of a probable second $\frac{1}{2}^+$ band. The dashed curve is the same as the solid curve for the $\frac{1}{2}^+$ state, but shifted by 8.5°.

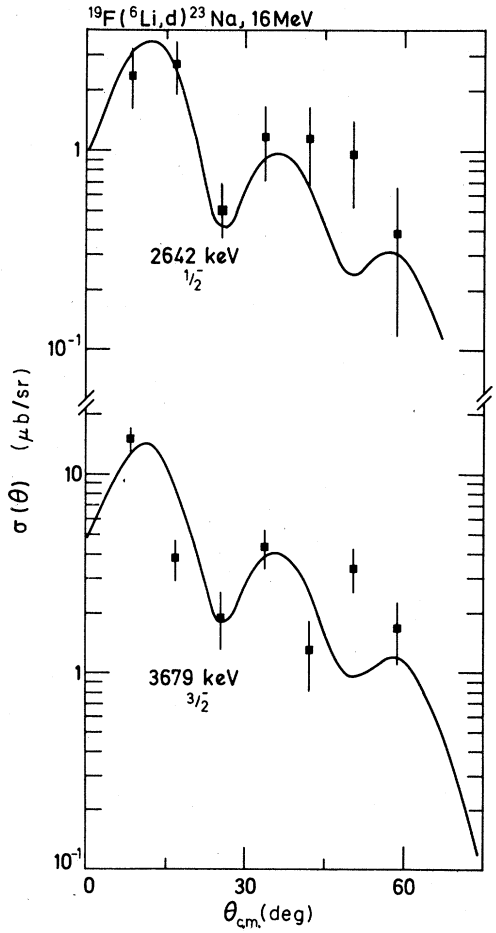

FIG. 6. Same as Fig. 3, but for first two members of $\frac{1}{2}^-$ band.

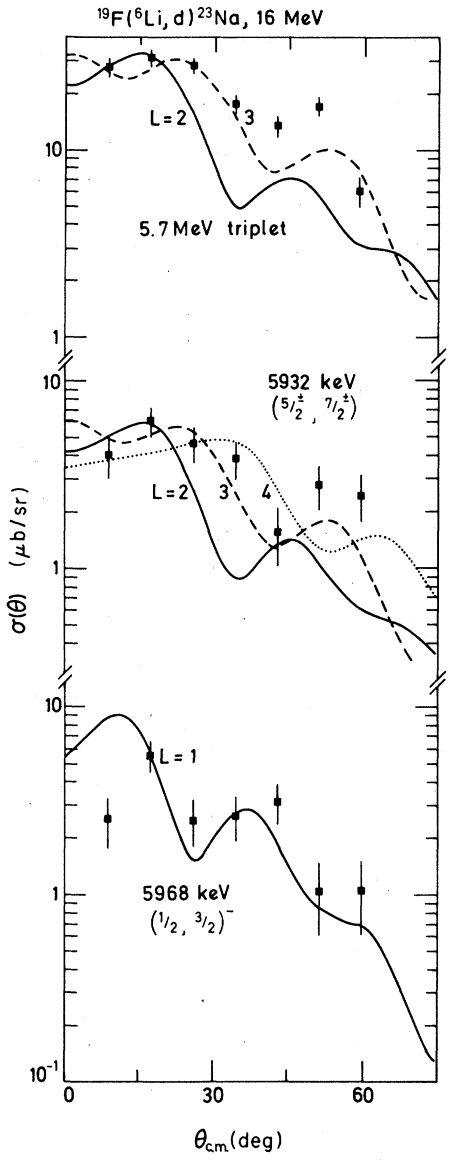

FIG. 7. Angular distributions for additional levels below 6 MeV excitation. Relative spectroscopic strengths $(2J+1)$ S are listed in Table IV.

later in this Section. It is surprising that the SU(3) calculations produce such poor agreement with the data. It is striking, though probably meaningless, that the experimental spectroscopic factors for the g.s. $K^{\pi}=\frac{3}{2}^{+}$ band are in very good agreement with the SU(3) predictions for the $K^{\pi}=\frac{1}{2}^{+}$ band of the $(\lambda\mu)=(83)$ configuration.

Angular distributions for members of the first $\frac{1}{2}^{+}$ band are displayed in Fig. 4. This band is thought to correspond predominantly to the configuration of the odd particle in N.O.9. We have identified this band with the $\frac{1}{2}^{+}$ band of the $(\lambda\mu)=(83)$ structure because it should lie lower. However, the $\frac{1}{2}^{+}$ member of the $(\lambda\mu)=(83)$ $\frac{1}{2}^{+}$ band has no α strength, so that the spectroscopic factor observed for the $\frac{1}{2}^{+}$ state must be due to admixtures of other SU(3) representations, in particular (64). The extracted spectroscopic factor for this $\frac{1}{2}^{+}$ state is not very reliable because of the poor fit to its angular distribution. This is a consistent problem observed in the present work. The $L=0$ DWBA curves are not in phase with the data for $\frac{1}{2}^{+}$ states. Nevertheless, S_{α} for the 2.39-MeV state must be large. It has the largest cross section of any state observed below 6 MeV excitation. The SU(3) calculations predict a large S_{α} for the $\frac{1}{2}^{+}$ member of the $(\lambda\mu)=(64)$ configuration.

The $L=2$ and 4 DWBA curves for the $\frac{3}{2}^{+}$ and $\frac{7}{2}^{+}$ members, respectively, of this band are in excellent agreement with the data. The $\frac{5}{2}^{+}$ member is unresolved from a nearby $\frac{5}{2}^{-}$ state, but the $\frac{5}{2}^{-}$ contribution appears to be small. The observation of comparable spectroscopic factors for the $\frac{3}{2}^{+}$ and $\frac{5}{2}^{+}$ members of this band is not consistent with the SU(3) predictions for the (83) $\frac{1}{2}^{+}$ band. Also, the predicted strength for the $\frac{3}{2}^{+}$ state is much greater than that observed. The observed strength of the $\frac{7}{2}^{+}$ state is far below the predicted strength for the $\frac{7}{2}^{+}$ state with $(\lambda\mu)=(83)$. The theoretical spectroscopic factor for the $\frac{7}{2}^{+}$ member of the $(\lambda\mu)=(64)$ $\frac{1}{2}^{+}$ band is very small ($S_{\alpha}=0.28$) and mixing might reproduce the data. The experimental counterpart of this $\frac{7}{2}^{+}$ state is not known.

Angular distributions for a second $\frac{1}{2}^{+}$ state and

TABLE III. Optical-model parameters used in DWBA calculations.

Channel	V_0 (MeV)	$r_0=r_{so}$ (fm)	$a_0=a_{so}$ (fm)	W'[a] (MeV)	r'_0 (fm)	a' (fm)	V_{so} (MeV)	r_c (fm)
^{19}F + ^{6}Li	−35.5	1.42	0.92	38	1.71	0.89	0	1.48
^{23}Na + d	−105.0	1.02	0.86	87[b]	1.42	0.65	−6.0	1.30
Bound state		2.10	0.60				0	2.10

[a] $W'=4W_D$.

[b] In the deuteron channel $W'=87-2.0E_x$.

a probable $\frac{5}{2}^+$ state are displayed in Fig. 5. These states have been suggested[3] as the $\frac{1}{2}^+$ and $\frac{5}{2}^+$ members of a second $\frac{1}{2}^+$ band. The problem of fitting angular distributions for $\frac{1}{2}^+$ states is again apparent here. The $L=2$ fit for the 5.38-MeV $\frac{5}{2}^+$ state is only fair. This second $\frac{1}{2}^+$ state is much weaker than the lower one, contrary to what one would expect if it were dominantly the $\frac{1}{2}^+$ member of the $(\lambda\mu)=(64)$ configuration. The measured spectroscopic factor for the 5.39-MeV state is significantly less than that predicted for the $\frac{5}{2}^+$ member of this band. In fact, relative to the g.s., all of the $\frac{5}{2}^+$ states are much weaker than predicted. (We return to this point later.) Of course, this second $\frac{1}{2}^+$ band might correspond to the $\frac{1}{2}^+$ band of the configuration $(\lambda\mu)=(45)$, all of whose members are predicted to be weak. This is, however, very unlikely as the mixed-configuration shell model (see below) predicts no such state below ~10 MeV excitation.

Angular distributions for the $\frac{1}{2}^-$ and $\frac{3}{2}^-$ states are displayed in Fig. 6. The $\frac{1}{2}^-$ state is very weak (as expected for a hole state) and difficult to separate from the nearby $\frac{9}{2}^+$ state. Nevertheless, an $L=1$ curve gives a reasonable fit. The $\frac{3}{2}^-$ state is somewhat stronger and its angular distribution is slightly more forward peaked than is the DWBA curve. Spectroscopic factors for the two states are comparable and small—indicating at most a small amount of $(1f2p)$ shell excitation. This is consistent with the ^{22}Ne(^{3}He, d) results, which obtained very small proton strengths for these two states. The $\frac{5}{2}^-$ member of this band, at 3.85 MeV, is unresolved from the $\frac{5}{2}^+$ state at 3.92 MeV, but the combined angular distribution indicates little $L=3$ strength.

Angular distributions for additional states below 6 MeV (listed in Table IV) are displayed in Fig. 7. These correspond[7] to an unresolved triplet of states near 5.7 MeV and a pair of states between 5.9 and 6.0 MeV. In ^{22}Ne(^{3}He, d) (Ref. 3) a state at 5.740 MeV had an $l=2$ angular distribution and a proton spectroscopic factor comparable to that for the $\frac{5}{2}^+$ state at 3.92 MeV. The 5.74-MeV state was suggested as a candidate for the band head of a $K^\pi=\frac{5}{2}^+$ band built on N.O.5, but its proton strength was significantly less than predicted. States at 5.76 and 5.78 MeV are thought[5] to have low spin, $J=\frac{1}{2}$ or $\frac{3}{2}$. In (^{3}He, d), the combined angular distribution for the two states was intermediate between that for $l=1$ and $l=2$.

In the present work, the combined angular distribution of the 5.7-MeV group is not very well described by an $L=2$ curve. But if one member is a $\frac{5}{2}^+$ state it could contain appreciable strength and might account for some of the missing $\frac{5}{2}^+$ strength for lower states. However, its strength is still significantly less than that predicted for the $\frac{5}{2}^+$ bandhead of the $(\lambda\mu)=(45)$ configuration, which is the only other $\frac{5}{2}^+$ state predicted to be strong.

Two states are known to exist at 5.93 and 5.97 MeV. The latter has[4] an $l=1$ angular distribution in proton pickup, implying $J^\pi=\frac{1}{2}^-$ or $\frac{3}{2}^-$. In a ^{25}Mg(d,α) study (Ref. 5), $\frac{1}{2}^-$ is preferred. In either case, it would have $L=1$ in (^{6}Li, d). An $L=1$ curve gives a reasonable fit to the data. The 5.93-MeV level is suggested[5] in ^{25}Mg(d,α) to have $J=\frac{5}{2}$ or $\frac{7}{2}$, parity undetermined. The (^{6}Li, d) angular distribution for the 5.93-MeV state is best fitted by a large L value, $L=3$ or 4, consistent with the (d,α) results, but giving no further information on J^π.

We present in Table V for each J^π the summed α spectroscopic factors (both experimental and theoretical) for all the positive-parity states below 6 MeV, when S (g.s.) is set to unity for both experiment and theory. If we focus on those for $\frac{3}{2}^+$ and $\frac{5}{2}^+$, which are probably the most reliable, the summed theoretical strengths for both are about 2.5 times the respective experimental val-

TABLE IV. ^{19}F(^{6}Li, d)^{23}Na results for additional levels.

Group[a]	E_x (MeV)[a]	Literature E_x (MeV)[b]	J[b]	$N-1;L$	$(2J_+ + 1)S_\alpha$[d] (rel)
14		5.741	$(\frac{3}{2},\frac{5}{2})^+$	3;2	4.4
15	5.7	5.766	···	2;3	3.1
16		5.781	···[c]	4;0	2.2
17	5.932	5.931	$\frac{5}{2}$ or $\frac{7}{2}$	3;2	0.83
				2;3	2.1
				2;4	2.5
18	5.968	5.967	$(\frac{1}{2},\frac{3}{2})^-$	3;1	1.2

[a] Reference 3.
[b] Reference 7.
[c] Reference 5.
[d] Same normalization as Table II.

ues. This would indicate the g.s. has obtained α strength through mixing with higher $\frac{3}{2}^+$ states, and that better overall agreement would have been obtained with a different relative normalization between experiment and theory. This is even more apparent if we sum the strengths for each L value, rather than each J. It is perhaps not surprising that pure SU(3) calculations fail to account for the mixing of α strength among states of the same J, considering the high degree of coherence involved. But it is surprising that while accounting roughly for the summed strength of each L, the splitting between states with $J = L + \frac{1}{2}$ and $J = L - \frac{1}{2}$ for $L = 4$ and 6 is so poorly reproduced.

Realistic shell-model calculations do no better. We present in Table VI the predicted S_α's from a truncated $(sd)^7$ shell-model calculation using the Preedom-Wildenthal[13] residual interaction matrix elements. The truncation was especially suited for the calculation of spectroscopic amplitudes as it kept all low-lying SU(3) representations $(\lambda\mu)$ which have overlap with $\alpha + {}^{19}\mathrm{F}(60)$. These include $(\lambda\mu) = (83)$ and (64). The next most important representation, (45), was a negligible component (<1%) in the five lowest eigenstates of $J = \frac{1}{2}$, $\frac{3}{2}$, and $\frac{5}{2}$. In fact any band with dominant (45) symmetry must start higher than ~10 MeV excitation. The various K_L values allow up to 7 configurations in some states, fewer in others, but only those with even L will contribute to S_α. The wave functions for the members of the ground state band are given in Table VII. As seen from Table VI, the calculations reproduce very well the excitation energies of the g.s. band, despite the severe truncation. [For $J = \frac{5}{2}$ the dimensionality in this calculation was 43, compared with 1142 in the full $(sd)^7$ space.] The wave functions for the g.s. band are fairly mixed, as can be seen from Table VII. The leading SU(3) representation, $(\lambda\mu) = (83)$ with $K_L = 1$, constitutes about 75% of the wave function for each member of the g.s. band.

Unfortunately, the additional coherence brought in by the major admixed components is such as to make agreement between the experimental and theoretical S_α's worse. The experimental values in Table VI have been multiplied by the factor 2.5 deduced above to make the summed strengths agree better. But for every state in the g.s. band, the shell model S_α's are in poorer agreement with experiment than are those for the pure (83) $K_J = \frac{3}{2}$ band, despite the fact that the levels of ^{23}Na are not very well described by the pure SU(3) model.

It is interesting to note from Table VI that the energies of the members of the first $K^\pi = \frac{1}{2}^+$ band are quite well predicted also, after a band shift of ~1 MeV has been carried out. Such band shifts have been observed before[14] in this mass region.

TABLE V. Summed spectroscopic factors for positive-parity states below 6 MeV.

	Summed strength			Summed strength		
J^π	Exp.	SU(3)	L	Exp	SU(3)	Exp. $\times$ 2.5
$\frac{1}{2}^+$	(4.5)	6.67	0	(4.5)	6.67	(11)
$\frac{3}{2}^+$	1.85	4.52	2	4.71[a]	12.79	11.8
$\frac{5}{2}^+$	2.86[a]	8.27				
$\frac{7}{2}^+$	3.42	2.57	4	4.08	8.40	10.2
$\frac{9}{2}^+$	0.66	5.83				
$\frac{11}{2}^+$	(1.8)	0.89	6	(1.8)	3.56[b]	(4.5)

[a] Includes S_α for probable $\frac{5}{2}^+$ state at 5.74 MeV.

[b] Includes predicted S_α for $\frac{13}{2}^+$ state.

TABLE VI. Comparison of experimental and shell-model results.

		E_x (MeV)		S (rel)	
K	J	Exp.	s.m.[a]	Exp[b]	s.m.[a]
$\frac{3}{2}^+_1$	$\frac{3}{2}^+$	0.0	0.0	2.5	1.0
	$\frac{5}{2}^+$	0.44	0.65	1.0	5.1
	$\frac{7}{2}^+$	2.08	2.03	5.0	0.8
	$\frac{9}{2}^+$	2.70	3.03	3.5	8.4
	$\frac{11}{2}^+$	5.54	5.05	(4.6)	0.03
	$\frac{13}{2}^+$	6.23	6.23	···	7.4
	$\frac{15}{2}^+$		8.89		
	$\frac{17}{2}^+$		10.51		
$\frac{1}{2}^+_1$	$\frac{1}{2}^+$	2.39	2.34[c]	10.0	2.6
	$\frac{3}{2}^+$	2.98	2.72	2.5	8.6
	$\frac{5}{2}^+$	3.91	3.85	(2.8)	0.06
	$\frac{7}{2}^+$	4.78	4.84	3.5	1.4
	$\frac{9}{2}^+$	(6.58)	6.43		0.16
	$\frac{11}{2}^+$		8.27		0.61
	$\frac{13}{2}^+$		10.09		0.05
$\frac{1}{2}^+_2$	$\frac{1}{2}^+$	4.43	6.80	1.4	6.4
	$\frac{5}{2}^+$	5.38	7.38	0.85	4.8
	$\frac{3}{2}^+$		10.75		0.88
$\frac{5}{2}^+_1$	$\frac{5}{2}^+$		6.01		0.04
	$\frac{7}{2}^+$		7.20		0.01
	$\frac{9}{2}^+$		8.55		1.14

[a] Shell-model calculation, as described in text.

[b] Values from Table II have been multiplied by 2.5 to give better agreement with summed strengths.

[c] A band shift of +1 MeV has been applied to the calculated states.

TABLE VII. Wave functions for members of the ground state rotational band of ^{23}Na. In addition, the states of the ground state band contain (typically) 10% [421] (91) and smaller amounts of [421] (72) and (64). The only other representations which can contribute to the α-transfer strength, i.e., [43] (45) and (26), are negligible ($\ll$1%) components of low-lying states. The (91) representation can contribute only via the small admixtures of [21] (41) in the ^{19}F ground state. These have not been taken into account but estimates show they are very small, not enough to affect the conclusions.

	(83) $K_L=1$		(83) $K_L=3$				
J^π	L^-	L^+	L^-	L^+	(64) $K_L=0$	(64) $K_L=2$	(64) $K_L=4$
$\frac{3}{2}^+$	0.7596	−0.4151	···	···	−0.0258	0.3497	···
$\frac{5}{2}^+$	0.6949	−0.5000	(0)	0.0345	0.1549	0.1635	···
$\frac{7}{2}^+$	0.7911	−0.3656	0.0345	0.0418	0.0456	0.2257	0.0081
$\frac{9}{2}^+$	0.6835	−0.4840	0.0896	0.0126	0.2219	0.2476	0.0128
$\frac{11}{2}^+$	0.8484	−0.2105	0.0274	0.0551	0.1086	0.1107	0.0039
$\frac{13}{2}^+$	0.6534	−0.4431	0.2028	−0.0591	0.2755	0.3122	0.0517

However, the S_α's in this band are in only fair agreement with the predictions of the model.

The calculations predict at least three additional low-lying bands, with $K^\pi = \frac{1}{2}^+$, $\frac{5}{2}^+$, and $\frac{7}{2}^+$. The $\frac{7}{2}^+$ band, which also arises in untruncated[14] shell-model calculations, is not known experimentally and hence must lie higher than the predicted energy of ~4 MeV. This is presumably due to another band shift. The $\frac{1}{2}^+$ band is probably to be identified with the band beginning at 4.4 MeV. The state at 5.74 MeV (if indeed $\frac{5}{2}^+$) has been suggested[3] as the head of a $K^\pi = \frac{5}{2}^+$ band. The other members of this band lie higher than the cutoff of the present experiment.

In summary, single-representation SU(3) calculations produce poor agreement with α-spectroscopic factors measured with the reaction ^{19}F(^{6}Li, d)^{23}Na. Realistic shell-model calculations show a good deal of configuration mixing, but do *not* improve the agreement between measured and calculated S_α's. The source of the poor agreement is not understood. It is unlikely that increasing the size of the basis will change the calculated S_α's by more than ~25%. It would therefore be interesting to perform the same reaction at a higher bombarding energy to see if the S_α's change.

The calculations were carried out with Dr. D. J. Millener's shell model codes, and A. P. wishes to thank him for his help.

*Present address: KVI, Groningen, on leave from University of Pennsylvania.

†Present address: IDA, 400 Army-Navy Drive, Arlington, Virginia 22202.

‡Present address: Institut für Kernphysik der Johann Wolfgang Goethe-Universität, Frankfurt a.M., Germany.

[1]N. Anantaraman, H. E. Gove, J. P. Trentelman, J. P. Draayer, and F. C. Jundt, Nucl. Phys. A276, 119 (1977); N. Anantaraman, H. E. Gove, J. Toke, and J. P. Draayer, *ibid.* A279, 474 (1977); N. Anantaraman, J. P. Draayer, H. E. Gove, and J. P. Trentelman, Phys. Rev. Lett. 33, 846 (1974); J. P. Draayer, H. E. Gove, J. P. Trentelman, N. Anantaraman, and R. M. De Vries, Phys. Lett. 53B, 250 (1974); N. Anantaraman, H. E. Gove, J. Toke, and J. P. Draayer, *ibid.* 60B, 149 (1976).

[2]H. W. Fulbright *et al.*, Nucl. Phys. A284, 329 (1977).

[3]J. R. Powers, H. T. Fortune, R. Middleton, and O. Hansen, Phys. Rev. C 4, 2030 (1971).

[4]J. D. Sherman, O. Hansen, J. R. Powers, and H. T. Fortune, Nucl. Phys. A257, 45 (1976).

[5]J. R. Powers, H. T. Fortune, and R. Middleton Nucl. Phys. A298, 1 (1978).

[6]G. G. Frank, R. V. Elliott, R. H. Spear, and J. A. Kuehner, Can. J. Phys. 51, 1155 (1973); D. E. Gustafson, S. T. Thornton, T. C. Schweizer, J. L. C. Ford, Jr., P. D. Miller, R. L. Robinson, and P. H. Stelson, Phys. Rev. C 13, 691 (1976); G. J. Ke Kelis, A. H. Lumpkin, K. W. Kemper, and J. D. Fox, *ibid.* 15, 664 (1977); J. Gomez del Campo *et al.*, *ibid.* 12, 1247 (1975).

[7]P. M. Endt and C. vander Leun, Nucl. Phys. A214, 1 (1973).

[8]J. Dubois, Nucl. Phys. A104, 657 (1967); G. G. Frank, M. W. Greene, D. T. Kelly, A. A. Pilt, and J. A. Kuehner, Phys. Rev. Lett. 28, 571 (1972).
[9]J. P. Draayer, Nucl. Phys. A237, 157 (1975).
[10]R. Middleton, in *Proceedings of the Fifth International Conference on Nuclear Reactions Induced by Heavy Ions, Heidelberg, Germany, 1969*, edited by R. Bock and W. R. Hering (North-Holland, Amsterdam, 1970), p. 263.
[11]P. D. Kunz (private communication).
[12]K. Bethge, M. Fou, and R. Zurmuhle, Nucl. Phys. A123, 521 (1969).
[13]B. M. Preedom and B. H. Wildenthal, Phys. Rev. C 6, 1633 (1972).
[14]B. J. Cole, A. Watt, and R. R. Whitehead, J. Phys. G 3, 303 (1975).